Advances in Machinery, Materials Science and Engineering Application
M. Chen et al. (Eds.)

doi:10.3233/ATDE220435

Effect of Retrogressions on Precipitation Characteristics and Strength Property in an Al-Zn-Mg-Cu Alloy

Weicai REN [a,c,d], Xiwu LI [a,b,c], Kai WEN [a,b,c 1], Yongan ZHANG [a,b,c,2], Xinyu LV [d] and Baiqing XIONG [a,c]

[a] *State Key Laboratory of Non-ferrous Metals and Processes, GRINM Group Co., LTD., Beijing 100088, China*
[b] *GRIMAT Engineering Institute Co., LTD., Beijing 101407, China*
[c] *General Research Institute for Nonferrous Metals, Beijing 100088, China*
[d] *Northeast Light Alloy Co., LTD., Harbin 150060, China*

Abstract. Retrogression treatment is a crucial process to obtain preferential microstructure and mechanical property for aviation Al-Zn-Mg-Cu alloys. In the current work, ramping time, preservation time and temperature were set as variations to investigate property evolution and precipitation characteristics for a commercial Al-Zn-Mg-Cu alloy. The results showed that the strength exhibited a continuously decrease trend with the enhancement of preservation temperature or the extension of preservation time. For a same strength level with different preservation temperature and time matches, GPII zone and η' phase were detected as the main types of precipitates, which showed apparent coherency and semi-coherency with the matrix, respectively. Phases with relatively large size possessed larger proportions for higher preservation temperatures while the average grain size exhibited an increase trend. As for prolonging ramping time, similar strength degradation was observed under equivalent preservation regimes. For the same strength level with different ramping and preservation time matches, the precipitates were still GPII zone and η' phase. With the prolonging of ramping time, the proportion of phases with relatively large size exhibited a decrease trend, so as to the average grain size (AGS). The subtle differences of precipitation characteristics and strength property matches were analyzed, which provided a promising way to improve overall performance of Al-Zn-Mg-Cu alloys.

Keywords. Retrogression, precipitation, strength property, Al-Zn-Mg-Cu alloy

1. Introduction

After nearly a century of development, Al-Zn-Mg-Cu alloys have gradually become the mainstream material for aerospace and military fields due to preferential unions of strength, fatigue crack growth, fracture toughness and stress corrosion cracking (SCC)

[1] Kai Wen, Corresponding author, GRIMAT Engineering Institute Co., LTD., No. 11 Xingke East Street, Yanqi Economic Development Zone, Huairou Street, Beijing 101407, P. R. China; E-mail: wenkai@grinm.com.

[2] Yongan Zhang, Corresponding author, GRIMAT Engineering Institute Co., LTD., No. 11 Xingke East Street, Yanqi Economic Development Zone, Huairou Street, Beijing 101407, P. R. China; E-mail: zhangyongan@grinm.com.

resistance [1-4]. During the complicated fabrication processes, aging treatment is a vital pass to obtain suitable microstructure characteristics and preferential overall performance [5,6]. Abundant researchers have paid attention to adjusting aging regimes, single stage peak-aging regimes for supreme strength, double stage over-aging regimes for good corrosion property and retrogression and re-aging (RRA) regimes for high strength and good fracture and corrosion properties [7-9]. Among them, RRA treatment is regarded as the most effective way to simultaneously obtain nearly peak strength, preferential resistance on SCC, fracture toughness and fatigue property [10,11].

Lots of researches have proved that retrogression part plays an important role, which should be investigated in detail. Thereinto, ramping time, preservation time and temperature are all responsible for final microstructure and property [12]. Higher preservation temperature leads to faster growth and coarsening of precipitates, leading to apparent strength degradation and improvement of fracture or corrosion property. Similar phenomenon can be observed by prolonging preservation time. As for ramping time, its effect is correlated to subsequent preservation ones. Although RRA regimes have been investigated detailedly for the advantage on other aging treatments, the subtle adjustment on above three factors to obtain optimal overall performance for specific alloys is not clear, especially for commercial Al-Zn-Mg-Cu alloys.

In the present study, a commercial Al-Zn-Mg-Cu alloy thick plate is employed and ramping time, preservation time and temperature of retrogression parts are fully adjusted to investigate precipitation and property evolution. The correlations between precipitation characteristics and property matching are analyzed and discussed.

2. Experimental Procedure

The experiments were implemented on a commercial Al-Zn-Mg-Cu alloy pre-stretching thick plate with a thickness of 3 inches, which had a composition of Al-6.2Zn-2.3Mg-2.2Cu-0.1Zr-0.05Fe-0.04Si (wt.%). Samples for precipitation observation and tensile property tests were cut from the center of thickness within a width range from a quarter to half of the plate width. Samples were heat treated in electro-thermostatic blast ovens with a temperature range of 1 ℃. A regime of 120℃/24h was chosen as the first and third stage regimes of RRA aging treatment. As for second stage regimes, samples were preserved at 170℃, 175℃ and 180℃ for different times with a same ramping time of 1h50min. Besides, ramping times of 2h50min and 3h50min were investigated with a second stage preserving temperature of 175 ℃. Ultimate tensile strength (UTS) was measured on a universal tensile testing machine from Metex Industrial Systems Co., LTD, which had a maximum load of three tons and a tensile speed of two millimeters per minute. The test process met ASTM E517 standard and yield strength was measured by an extensometer attached to the machine. The elongation was measured from fractured specimens. Precipitation types and geometrical characteristics with different aging treatments were observed by a Talos F200X transmission electron microscope (TEM) machine. The TEM observation samples were extracted from heat treated specimens, which were artificially milled to slices with a thickness of 50-60μm. Then the slices were electropolished under a temperature range of -30 to -40℃ cooled with liquid nitrogen by a double jet thinners. The corrosive liquid contained nitric acid and methanol and the matching was 1:3. The sizes of matrix precipitates were measured by an image processing software (Image Pro Plus) on related TEM graphs.

3. Results and Discussion

3.1. Match of Preserving Temperature and Time for different Retrogression Regimes

On the basis of a ramping time of 1h50min, the alloy is retrogressed at 170℃, 175℃ and 180℃ for different times, the corresponding tensile property is show in figure 1. It is clear that both ultimate tensile strength (UTS) and yield strength (YS) show a decrease trend for different retrogression temperature with the prolonging of retrogression time while the elongations exhibit an increase trend. For a preservation time of 1.5h, the UTS and YS for different preservation temperature are almost the same, with a value range of 607-611MPa. The preservation temperature is higher, the degradation of strength is quicker. When the alloy is preserved for 7.5h under different times, the UTS for them are 565MPa, 551MPa and 517MPa, successively. The YS show a similar trend. Meanwhile, the elongations show no obvious trend. Here we can see that the alloy can reach a certain strength level for different preservation temperatures matching suitable times. Table 1 gives different regimes for the alloy with an UTS level of 560-565MPa, it can be perceived that retrogression regimes of 170℃/7.5h, 175℃/6.5h and 180℃/4.5h possess approximate tensile property.

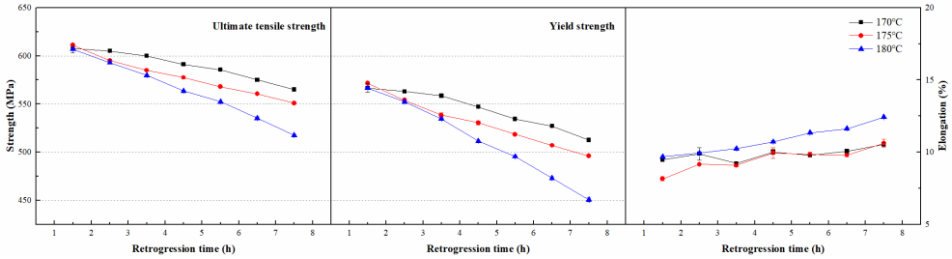

Figure 1. Ultimate tensile strength, yield strength and elongation of the alloy treated by 120℃/24h+(170,175,180)℃/ ***x*** h+120℃/24h.

Table 1. Tensile property of the alloy with different retrogression regimes under a same strength level.

Aging regimes	R_m (MPa)	$R_{p0.2}$ (MPa)	A (%)
120℃/24h+170℃/7.5h+120℃/24h	565	513	10.5
120℃/24h+175℃/6.5h+120℃/24h	561	507	9.8
120℃/24h+180℃/4.5h+120℃/24h	563	512	10.7

In order to furtherly investigate the disparity of various preserving temperature and time matches, precipitation types are identified by selected area diffraction patterns (SADPs) from the $<100>_{Al}$ and $<112>_{Al}$ orientations, as showed in figure 2. The main diffraction spots and rays projected from the α(Al) matrix have been identified. Some weak but distinct spots are revealed near a half of {311} positions in $<112>_{Al}$ orientation, which represent GPII zone. The spots and rays at 1/3{220} and 2/3{220} position from the $<100>_{Al}$ and $<112>_{Al}$ orientations, respectively, come from semi-coherent η' phase. Besides, spots of Al_3Zr phase are found at {010} position in $<112>_{Al}$ orientation. Here we can see that precipitation types for various retrogression regimes are the same, namely, the GPII zone and η' phase possess the majority.

Based on the SADPs analysis, high resolution TEM (HREM) images of precipitates are investigated. Figure 3 present HREM images of GPII zone and η' phase

of the alloy treated by 120°C/24h+175°C/6.5h+120°C/24h. It can be seen that both GPII zone and η' phase have elongated shapes while the latter one possesses larger size and thickness. The inverse FFT image of GPII zone reveals its coherency with the matrix. Meanwhile, part of η' phase exhibits lattice distortion, which reveals that η' phase is semi-coherent with the matrix. It needs to be pointed that the HREM morphology of GPII zone and η' phase for the rest two regimes are almost the same, which are not repeated here.

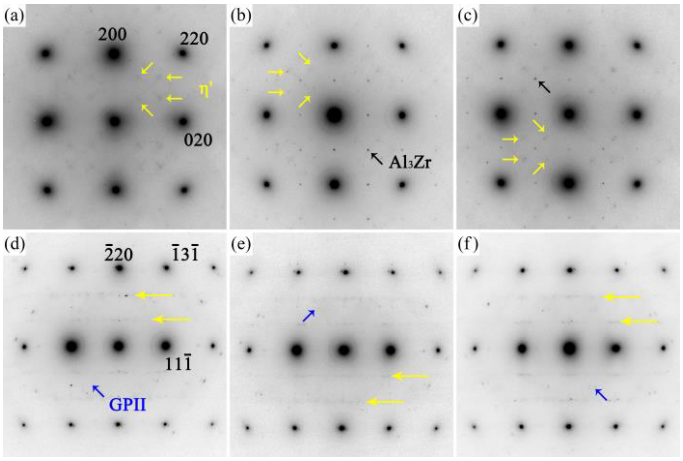

Figure 2. Selected area diffraction patterns (SADPs) along $<100>_{Al}$ and $<112>_{Al}$ orientations of the alloy with different retrogression regimes under a same strength level. (a,d) 120°C/24h+170°C/7.5h+120°C/24h, (b,e) 120°C/24h+175°C/6.5h+120°C/24h, (c,f) 120°C/24h+180°C/4.5h+120°C/24h.

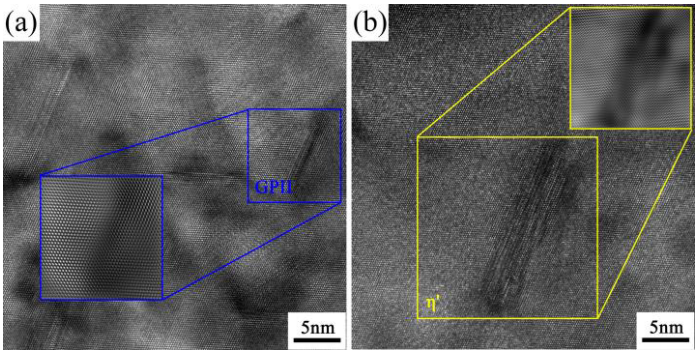

Figure 3. High resolution TEM images of precipitates and related inverse FFT images of the alloy with a regime of 120°C/24h+175°C/6.5h+120°C/24h. (a) GPII zone, (b) η' phase.

Based on the identification of phase types, precipitation characteristics are revealed by bright field TEM images, as shown in figure 4. In terms of matrix precipitates, it can be seen that the phases possess discal or elongated morphology, which can be explained by the relative direction along $<110>_{Al}$ orientation. The size of precipitates shows abundant variety, both coarse precipitates with large size and fine precipitates can be observed. As for grain boundary precipitates, typical features with discontinuous distribution are observed for different retrogression regime and the size of them show coarsen characteristics.

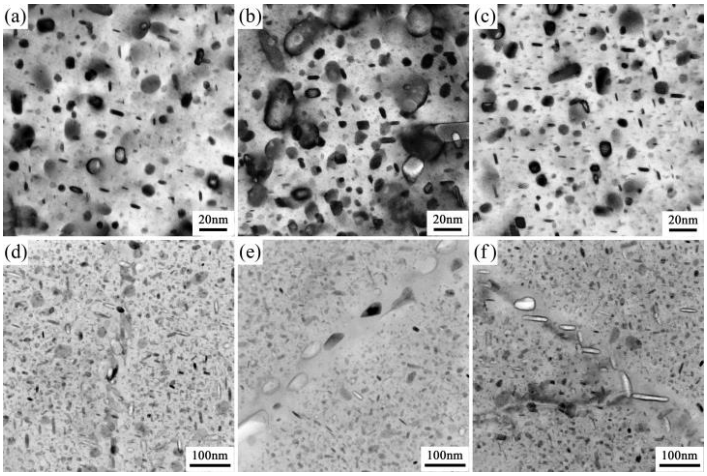

Figure 4. Precipitation characteristics of the alloy with different retrogression regimes under a same strength level. (a, d) 120°C/24h+170°C/7.5h+120°C/24h, (b, e) 120°C/24h+175°C/6.5h+120°C/24h, (c, f) 120°C/24h+180°C/4.5h+120°C/24h, (a, b, c) matrix precipitates, (d, e, f) grain boundary precipitates.

In order to furtherly investigate the size characteristics for different retrogression regimes, the diameters of precipitates are measured and related quantity are calculated in terms of size percent with a gap of 2nm, as showed in figure 5. Here we can see that the phases with a size within 6nm possess a half for all the regimes and the proportion for larger precipitates severely shrinks. As for precipitates with a size larger than 12nm, only small proportions belong to them. Comparing the size distributions of different retrogression regimes, we can see that the proportion of precipitate with a size within 4nm show a decrease while the proportion of precipitate with a size range of 4-12nm increases with the retrogression regime varies from 170°C/7.5h to 175°C/6.5h to 180°C/4.5h. This means the size distribution moves towards large size precipitates. The average precipitate sizes are calculated, which are 6.2nm, 6.9nm and 8.2nm, successively.

To sum up, under a same strength level, retrogression regime with higher temperature and shorter time possesses relatively more larger size precipitates.

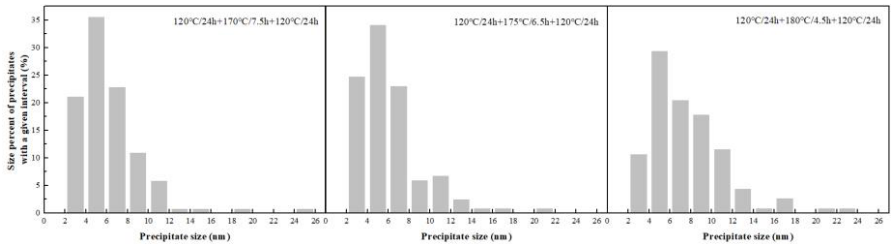

Figure 5. Precipitation size percent with a given interval of the alloy with different retrogression regimes under a same strength level.

3.2. Match of Ramping and Preserving times for Retrogression at 175°C

Based on the investigation of the matching of preservation temperature and time for retrogression regimes, ramping time is selected as a variation and the tensile property

of the alloy retrogressed at 175°C with different s ramping times is investigated, as shown in figure 6. Similarly, the UTS and YS show a decremental trend while the elongations show an opposite trend. Besides, the strength for the three ramping times with retrogressed for 1.5h is ordered as 1h50min>2h50min>3h50min, which is maintained for the prolonging of preservation time. In the same way, matches with different ramping and preservation times under a same UTS level are selected and related values are shown in table 2. It can be seen that retrogression regimes of (↑1h50min)175°C/6.5h, (↑2h50min)175°C/5.5h and (↑3h50min)175°C/4.5h reach a same UTS level of 560-562MPa.

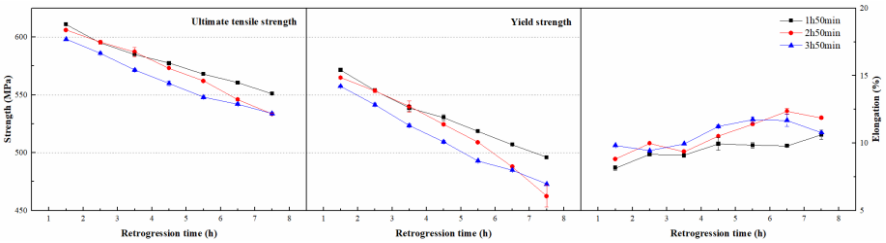

Figure 6. Ultimate tensile strength, yield strength and elongation of the alloy treated by 120°C/24h+175°C/ ***x*** h+120°C/24h with different ramping times.

Table 2. Tensile property of the alloy with different second stage ramping times under a same strength level.

Aging regimes	R_m (MPa)	$R_{p0.2}$ (MPa)	A (%)
120°C/24h+(↑1h50min)175°C/6.5h+120°C/24h	561	507	9.8
120°C/24h+(↑2h50min)175°C/5.5h+120°C/24h	562	509	11.4
120°C/24h+(↑3h50min)175°C/4.5h+120°C/24h	560	510	11.2

Because the microstructure characteristics of the alloy with a retrogression regime of (↑1h50min)175°C/6.5h have been detailedly investigated in previous part, only the other two are investigated here. Figure 7 exhibits SADPs of them, which reveal the main precipitates are also GPII zone and η' phase. Figure 8 shows matrix and grain boundary precipitates, the former one also possesses discal and elongated shapes while the latter one possesses discontinuous distributions.

The size distributions of the other two are also calculated and the results are shown in figure 9. Here we can see that the phases with a size within 8nm possess a half for all the regimes and the proportion for larger precipitates shrinks. As the prolonging of ramping time, it can be perceived that precipitates with relatively large size possess large proportions, which means the size distribution moves towards large size precipitates. The average precipitate sizes are calculated, which are 7.5nm and 8.5nm, successively, both are larger than 6.9nm for the ramping time of 1h50min.

To sum up, under a same strength level, retrogression regime with longer ramping time possesses relatively more larger size precipitates.

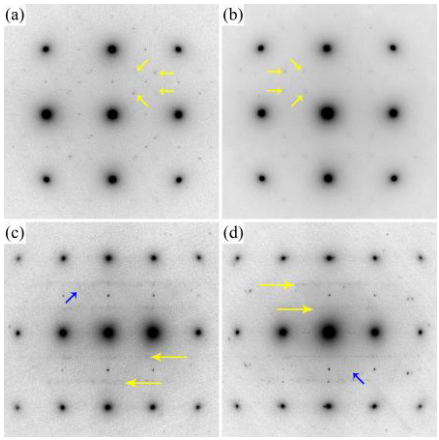

Figure 7. Selected area diffraction patterns (SADPs) along <100> and <112> zone of the alloy with different second stage ramping times under a same strength level. (a,c) 120°C/24h+(↑2h50min)175°C/5.5h+120°C/24h, (b,d) 120°C/24h+(↑3h50min)175°C/4.5h+120°C/24h, (a,b) matrix precipitates, (c,d) grain boundary precipitates.

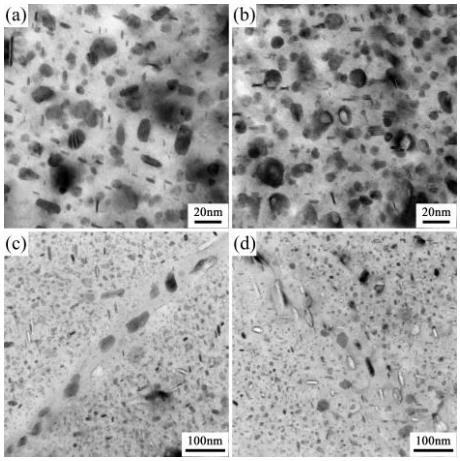

Figure 8. Precipitation characteristics of the alloy of the alloy with different second stage ramping times under a same strength level. (a,c) 120°C/24h+(↑2h50min)175°C/5.5h+120°C/24h, (b,d) 120°C/24h+(↑3h50min)175°C/4.5h+120°C/24h, (a,b) matrix precipitates, (c,d) grain boundary precipitates.

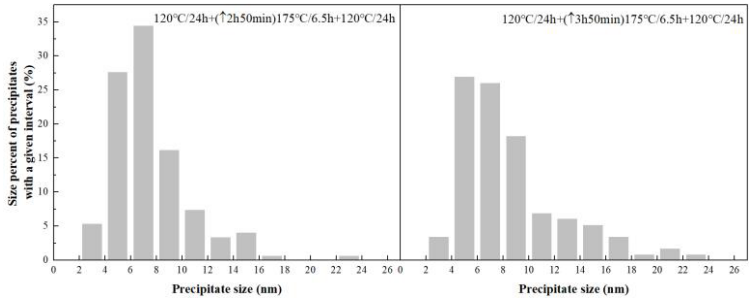

Figure 9. Precipitation size percent with a given interval of the alloy with different second stage ramping times under a same strength level.

4. Conclusion

In the present study, the precipitation characteristics and tensile property in an Al-6.2Zn-2.3Mg-2.2Cu alloy treated by RRA treatments with various retrogression parameters are thoroughly investigated. The UTS and YS are reduced with the prolonging the retrogression time while the elongations show an incremental trend. For different matching of preserving temperature and time or ramping and preserving times, the main precipitates are GPII zone and η' phase, which possess coherency and semi-coherency with the matrix, respectively. The precipitate size distributions for all the regimes are broadly the same, precipitates with relatively small size possess a larger proportion. Under a same strength level, the matches of higher preservation temperature and shorter time or longer ramping time and shorter preservation time correspond to more larger size precipitates and lager average precipitate size.

Acknowledgements

This study was financially supported by National Key R&D Program of China (No. 2020YFF0218200) and other related projects.

References

[1] Williams JC, Starke EA. Progress in structural materials for aerospace. Acta Mater. 2003 Nov; 51(19): 5775-5799.
[2] Heinz A, Haszler A, Keidel C, Moldenhauer S, Benedictus R, Miller WS. Recent development in aluminium alloys for aerospace applications. Mater. Sci. Eng. A. 2000 Mar; 280(1): 102-107.
[3] Zhou B, Liu B, Zhang S. The advancement of 7XXX series aluminum alloys for aircraft structures: A review. Metals. 2021 Apr; 11(5): 718.
[4] Dursun T, Soutis C. Recent developments in advanced aircraft aluminium alloys. Mater. Des. 2014 Apr; 56: 862-871.
[5] Azarniya A, Taheri AK, Taheri KK. Recent advances in ageing of 7xxx series aluminum alloys: A physical metallurgy perspective. J. Alloy. Compd. 2019 Nov; 781: 945-983.
[6] Sigli C, De Geuser F, Deschamps A, Lépinoux J, Perez M. Recent advances in the metallurgy of aluminum alloys. Part II: Age hardening. CR Phys. 2018 Nov; 19(8): 688-709.
[7] Rometsch PA, Zhang Y, Knight S. Heat treatment of 7xxx series aluminium alloys—Some recent developments. T. Nonferr. Metal. Soc. 2014 Jul; 24(7): 2003-2017.
[8] Zhao H, Gault B, Ponge D, Ponge D, Raabe D. Reversion and re-aging of a peak aged Al-Zn-Mg-Cu alloy. Scripta Mater. 2020 Aug; 188: 269-273.
[9] Buha J, Lumley RN, Crosky AG. Secondary ageing in an aluminium alloy 7050. Mater. Sci. Eng. A. 2008 Sep; 492(1-2): 1-10.
[10] Zhou L, Chen K, Chen S, Ding Y, Fan S. Correlation between stress corrosion cracking resistance and grain-boundary precipitates of a new generation high Zn-containing 7056 aluminum alloy by non-isothermal aging and re-aging heat treatment. J. Alloy. Compd. 2021 Aug; 850: 156717.
[11] Sun R, Sun Q, Xie Y, Dong P, Chen Q, Chen K. Enhancing corrosion resistance of 7150 Al alloy using novel three-step aging process. T. Nonferr. Metal. Soc. 2016 May; 26(5): 1201-1210.
[12] Liu Y, Liang S, Jiang D. Influence of repetitious non-isothermal aging on microstructure and strength of Al-Zn-Mg-Cu alloy. J. Alloy. Compd. 2016 Dec; 689: 632-640.